Reversible Solvent Denaturation of Rabbit Muscle Pyruvate Kinase

Wolfgang Doster and Benno Hess*

ABSTRACT: The structural transitions of the tetrameric rabbit muscle pyruvate kinase induced by guanidine hydrochloride and urea are characterized by elastic and quasi-elastic light-scattering, sedimentation velocity, and intrinsic viscosity experiments as well as by protein fluorescence, circular dichroism, and enzymic activity measurements. The transition curves are shown to be reversible. We find a new pathway of unfolding which is different from that described in the literature: The first intermediate with increasing concentration of denaturant is a less compact and inactive tetramer which can be renatured if substrates are added. Dissociation of the tetramer results in an expanded dimer with a partial loss of the secondary structure. The final state is a completely disordered monomer. These intermediates are consistent with a domain structure of pyruvate kinase, as it was suggested by Stammers & Muirhead [Stammers, D. K., & Muirhead, H. (1975) *J. Mol. Biol. 95*, 213-225] on the basis of their X-ray data. Using Schellman's solvent denaturation model [Schellman, J. A. (1978) *Biopolymers 17*, 1305-1322], we calculate the free energies of stabilization of the folding-unfolding equilibrium.

Reversible protein denaturation experiments contribute to the understanding of protein folding and unfolding occurring during de novo synthesis and proteolytic degradation in cells. Such experiments further allow determination of the thermodynamic stability of the native and of intermediary states relative to a random-coil conformation. The X-ray structure of the protein can be used to explain the stability of the observed intermediates. Solvent denaturation has the advantage over pH or temperature denaturation that is usually leads to completely disordered products. Solvent denaturation also provides us with information concerning the linkage between protein structure and the protein-solvent interaction. The significance of this effect becomes evident if substrates change the surface properties of an enzyme and, vice versa, if changes of the solvent affect the binding constants of the protein ligands.

Most denaturation studies to date deal with small monomeric proteins (Creighton, 1978). However, many enzymes, especially if they have a regulatory function, are composed of several subunits, and therefore these studies have to be extended to include oligomeric proteins. In this case the role of association and dissociation which may be linked to folding and unfolding has to be investigated. In a preliminary study (Doster & Hess, 1978) we showed that the tetramer pyruvate kinase of rabbit muscle is a suitable candidate for a multiparameter study of physical changes occurring during denaturation of an oligomeric enzyme.

The subunit structure of pyruvate kinase has been examined by Steinmetz & Deal (1966), and various intermediates have been detected. These workers deduced from their sedimentation measurements that the native tetramer (9.1 S) dissociates with increasing urea concentration into compact and active dimers (7.2 S), compact but inactive monomers (3.6 S), and disordered monomers (1.9 S). Dissociation and deactivation of this enzyme by urea and guanidine hydrochloride (Gdn·HCl)[1] were shown to be overall reversible (Johnson et al., 1969). Furthermore the X-ray structure of the cat muscle enzyme is available (Stammers & Muirhead, 1975).

On the basis of these data, we investigated the equilibrium solvent denaturation and renaturation of rabbit muscle pyruvate kinase by measuring several structural parameters. In addition to the sedimentation values, the diffusion coefficient and the molecular radius of the enzyme were determined by quasi-elastic light scattering. Conformational changes and changes of the molecular weight can be distinguished by combining the diffusion coefficient and the sedimentation constant. An independent measure of the molecular weight is provided by the integrated light scattering intensity. Parallel measurements of the intrinsic viscosity, the protein fluorescence, the circular dichroism, and the enzymic activity allowed us to characterize the intermediates of unfolding and to test the reversibility of the transition curves.

We here describe the reversible process of unfolding and the influence of various ligands on the structure of the enzyme in the presence of urea and Gdn·HCl. This leads to a new interpretation of the intermediates of the folding-unfolding equilibrium. On the basis of reversible transition curves, we derive equilibrium constants by using Schellman's solvent denaturation model (1978).

Materials and Methods

(*a*) *Reagents.* Ultrapure Gdn·HCl and urea were purchased from Serva Feinbiochemica. Solutions of Gdn·HCl and urea were adjusted to the desired pH and used within 12 h. The denaturant concentrations were determined with an Abbé refractometer (Kielley & Harrington, 1960). Rabbit muscle pyruvate kinase (EC 2.7.1.40) from Boehringer Mannheim (sp act. at 25 °C: 200 units/mg) was dialyzed against 0.1 M potassium phosphate (pH 6.5), 0.03 M 2-mercaptoethanol, 20% glycerol or 0.1 M Tris-HCl, 0.001 M EDTA, and 0.03 M 2-mercaptoethanol at pH 8. A small volume of concentrated enzyme (10 mg/mL), which was initially dissolved in buffer containing no denaturant, was diluted to the desired denaturant concentration and reacted for at least 1 h before the measurements were done. The samples in urea also contained 0.1 M KCl. As a control of the equilibrium, some samples were dialyzed against the denaturant. The enzyme preparation exhibited only one band when subjected to electrophoresis in polyacrylamide gels.

† From the Max-Planck-Institut für Ernährungsphysiologie, Rheinlanddamm 201, 4600 Dortmund 1, West Germany. *Received June 4, 1980.* This work was supported by a NATO grant.

[1] Abbreviations used: Gdn·HCl, guanidine hydrochloride; Tris, tris(hydroxymethyl)aminomethane; EDTA, ethylenediaminetetraacetic acid; LDH, lactate dehydrogenase; NADH, reduced nicotinamide adenine dinucleotide; ADP, adenosine 5'-diphosphate; PEP, phosphoenolpyruvate.

0006-2960/81/0420-0772$01.00/0

For renaturation the protein solution containing 30 μg/mL enzyme was diluted by 0.1 or 0.2 molar units of denaturant at 0 °C and in the presence of 0.03 M freshly added 2-mercaptoethanol. At low denaturant concentrations (tetrameric state), renaturation was faster than the time needed for the dilution procedure (30 s). At intermediate denaturant concentrations (tetramer–dimer equilibrium), however, it took the enzyme up to 1 h to reach the final state.

(*b*) *Enzymic Assay.* The enzyme activity was determined by two different methods. First, a coupled assay procedure with lactate dehydrogenase was used immediately after dilution of the denaturant. Standard assays were run in the following medium: 10 mM ADP, 20 mM $MgSO_4$, 10 mM phosphoenolpyruvate, 0.3 mM NADH, and 0.05 mg/mL LDH. The reaction was initiated by the addition of 10 μL of pyruvate kinase–denaturant solution to 2 mL of assay medium. NADH absorption changes were recorded in an Eppendorf photometer. All experiments were carried out at 5 °C, where no reactivation is observed (Johnson et al., 1969). Additionally, the proton uptake of the enzymatic reaction was measured without diluting the denaturant in pH-stat equipment.

(*c*) *Light-Scattering Measurements.* Elastic and homodyne quasi-elastic light-scattering experiments were performed simultaneously by using the light of a 50-mW Spectra Physics NeHe laser (Model 125A). The scattered field was analyzed by a 48-channel correlator (Malvern Molecular Analyser System 4300), which computes values of the clipped intensity autocorrelation function. The correlator was interfaced to an Interdata 716 computer, giving immediate data processing. Scattering angles between 105° and 75° were applied to improve the accuracy of the data. The scattering cells were cleaned with chromic acid and methanol and flushed with the buffer (given above), which was filtered by a high-flow 0.6–0.22-μm Millipore filter. After cleaning, ~1.5 mL of protein denaturant solution was passed into the cell via a 0.45-μm Millipore filter in a series with a 0.22-μm Millipore filter. To eliminate the random loss of protein by filtration, we also added a carefully filtered denaturant solution directly to a dust-free protein sample for the intensity measurements. The final protein concentration was between 1 and 2 mg/mL. The cell was placed into the thermoelectric heating–cooling block. Square cells were used to minimize the stray light.

The average intensity of the Rayleigh line was measured at 90°. Intensity ratios were used to determine molecular weight ratios as a probe for changes of the quarternary structure. The tetrameric enzyme was taken as a reference state. This eliminates the need of optical calibration of the instrument. It was assumed that the virial contributions are small. This approximation is quite reasonable at protein concentrations of 1 mg/mL and if no absolute molecular weights are required. The molecular weight ratios were obtained from the intensity ratios by the use of eq 1 (Timasheff & Townend, 1970):

$$\frac{I_{av,90}}{I_{0,90}} = \frac{n^2(dn/dc)^2cM}{n_0^2(dn_0/dc_0)^2c_0M_0} \quad (1)$$

M is the molecular weight, n is the refractive index, dn/dc is the refractive index increment, and c is the protein concentration in mg/mL. I_{90} is the average scattered intensity at 90°. The index 0 refers to the reference state. The refractive indices of the protein solution were measured with an Abbé refractometer. It was assumed that the refractive index increments were the same for all states of aggregation (Noelken & Timasheff, 1967). The background scattering of the buffer and the buffer plus denaturant was subtracted. To reduce random aggregation, which could be a serious source of error, we did some of the experiments in glycerol and at 5 °C. Experiments carried out without glycerol yielded practically the same results but were often complicated by the presence of protein aggregates.

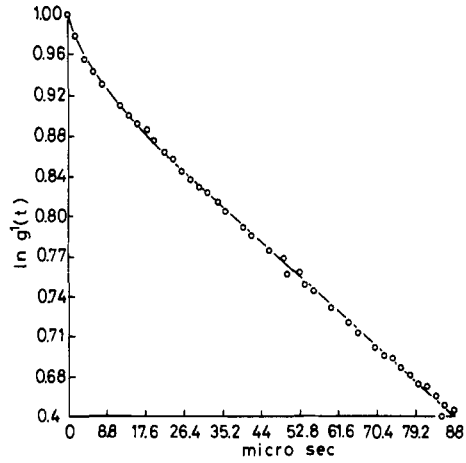

FIGURE 1: Normalized electric field autocorrelation function $g^1(t)$ and bimodal fit of pyruvate kinase (2 mg/mL) in phosphate buffer and 2.5 M Gdn·HCl (pH 6.5) at 5 °C. The scattering angle was 90°.

The principles of homodyne intensity fluctuation spectroscopy have been reviewed several times in the literature (Pusey et al., 1974). The autocorrelation function of the electric field scattered by diffusing macromolecules is given by (Cummins, 1973)

$$g^1(t) = \sum_i A_i \exp(-q^2D_it) \quad (2)$$

D_i is the translational diffusion coefficient of molecule i, A_i is an intensity factor, which is proportional to the concentration and the molecular weight of the molecules, and q is the magnitude of the scattering vector, $q = [4\pi n \sin(\theta/2)]/\lambda$, where θ is the scattering angle and λ is the laser wavelength. In our case $g^1(t)$ is analyzed as a sum of two exponentials by using a weighted procedure (Pusey et al., 1974), whereby the weight is proportional to $g^1(t)$.

The fitting of the experimental values was done in two steps. First, initial values were calculated and then secondly used for a nonlinear fitting program (Harwell-Subroutine VCO 5A) which was considerably improved by the initial values. The bimodal analysis was necessary because of the small but observable contribution of the denaturant to the spectrum. We obtained a diffusion coefficient for Gdn·HCl of $D_{20,w} = (70 \pm 20) \times 10^{-7}$ cm²/s, in agreement with a similar study of Dubin et al. (1973). The concentration dependence of the protein diffusion coefficient was negligable between 0.5 and 7 mg/mL.

Despite the presence of several macromolecular species in our system, no additional polydispersity was observed, because the corresponding diffusion coefficients differ by less than a factor of 2. This condition does not distort the Lorentzian shape of the spectrum, and only an average diffusion coefficient function is obtained (Dubin et al., 1973). A typical correlation function and a bimodal fit are shown in Figure 1.

The diffusion coefficient of the protein is related to the hydrodynamic radius of its equivalent sphere by the Stokes–Einstein formula:

$$D = KT/6\pi\eta R \quad (3)$$

The viscosity of the solvent η and the viscosity of the protein were measured with an Ubbelohde microviscosimeter (Schott AVS/G).

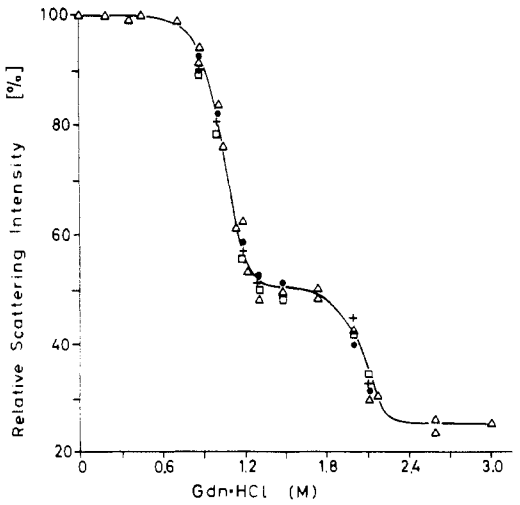

FIGURE 2: Relative scattering intensity at 90° of pyruvate kinase (2 mg/mL) in phosphate–glycerol buffer (pH 6.5) and Gdn·HCl at various temperatures: (△) 5, (●) 10, (+) 15, and (□) 20 °C. (—) Theoretical curve calculated from model 6.

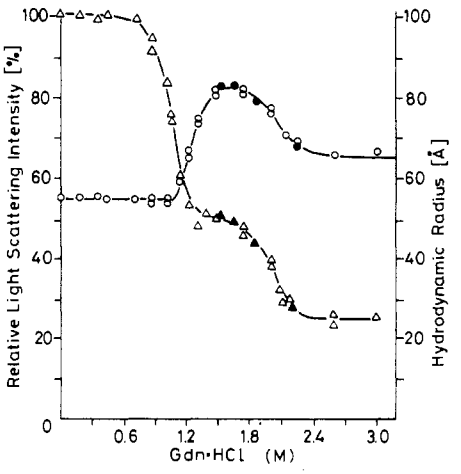

FIGURE 3: Relative scattering intensity (△) and hydrodynamic radius (○) in phosphate buffer (pH 6.5, 5 °C). (—) Theoretical curve obtained with the best parameter set of model 6. The open symbols are obtained by increasing the Gdn·HCl concentration; the filled symbols were obtained by decreasing the denaturant concentration.

(*d*) *Ultracentrifuge Measurements.* A Beckmann analytical ultracentrifuge with Schlieren optics was used for these studies. Sedimentation velocity experiments were run at 68 000 rpm near 10 and 20 °C. The protein concentration was 3.6 mg/mL.

(*e*) *Fluorescence.* Fluorescence measurements were made on a Perkin-Elmer MP-3 spectrophotometer equipped with a thermostated cell compartment. The protein was excited at 292 nm, and the fluorescence was observed between 300 and 350 nm. The fluorescence maximum was shifted from 335 to 340 nm with increasing denaturant concentration. For renaturation the protein denaturant solution was carefully diluted in small steps at 0 °C. Fresh mercaptoethanol was added.

(*f*) *Circular Dichroism.* A Jobin Yvon Dicrograph III was used to determine the ellipticity at the 222-nm extremum. The measurements were made at 5 °C and at a protein concentration of 0.5 mg/mL. The diameter of the sample cuvette was 0.1 cm.

Results

(*a*) *Elastic Light Scattering.* The molecular weight of the native system was found to be 237 000 (Steinmetz & Deal, 1966). Since the light scattered by a suspension of macromolecules is proportional to its average molecular weight (eq 1), the intensity ratio given in percent in Figure 2 is a measure of the average molecular weight of pyruvate kinase relative to the native state. Below 0.9 M Gdn·HCl no change of the molecular weight ratio is observed. At 1.1 M Gdn·HCl a sharp 50% decrease of the molecular weight occurs. This means, since the subunits of pyruvate kinase are identical, that a stable dimer is formed. A second sharp transition at 2.1 M Gdn·HCl, again a 50% decrease of the molecular weight, records the dissociation of the dimer into monomers. There is a small but hardly significant influence of the temperature on the transition curve. Therefore temperature effects are ignored in the discussion of the results.

(*b*) *Quasi-elastic Light Scattering and Sedimentation Velocity.* Figure 3 shows the hydrodynamic radius together with the molecular weight ratio as a function of the Gdn·HCl concentration. The values were obtained at pH 6.5 and 5 °C by either increasing (open symbols) or decreasing (closed symbols) the concentration of the denaturant. The figure indicates that only the dimer–monomer transition is reversible at the given protein concentration of 1 mg/mL (for the reversibility of the tetramer–dimer transition, see below). On further dilution of the denaturant below 1 M, incorrectly folded aggregates are formed for the given protein concentration. An explanation is obtained by considering the Stokes radius of the protein. The radius remains constant (55 Å) at low denaturation concentrations but increases markedly up to 84 Å between 1 and 1.5 M Gdn·HCl. In this concentration range, the tetramer dissociates into dimers, and a dissociation of compact molecules into smaller compact molecules should yield a decrease of the Stokes radius. This discrepancy is explained by changes of the protein structure resulting in an expanded state of dimer.

Between 1.9 and 2.3 M Gdn·HCl the radius decreases again to a level of 67 Å, corresponding to the formation of monomer. No further changes are observed at higher concentrations of denaturant.

For comparison of the various states defined in these experiments, the intrinsic viscosity of the protein was determined at three different denaturant concentrations. In the absence of denaturant the viscosity is 4.5 cm^3/g which is typical for a globular protein. The expanded state of the dimer at 1.5 M Gdn·HCl has a viscosity of 44 cm^3/g, and the monomer at 2.5 M Gdn·HCl has a value of 39 cm^3/g. These data are consistent with the values of the hydrodynamic radius.

The same combination of elastic and quasi-elastic light-scattering experiments were carried out as a function of the urea concentration at 5 °C and pH 6.5. Again a dissociation of the tetramer around 2.1 M urea runs in parallel with swelling and thus an increase of the Stokes radius. The values of 84 Å in Gdn·HCl and 86 Å in urea are consistent within the error of the measurements. As shown in Figure 4, urea is less efficient than Gdn·HCl but induces the same structural changes.

Summarizing, no evidence for a compact dimeric intermediate either in Gdn·HCl or in urea at pH 6.5 was obtained. A similar conclusion is derived from the sedimentation velocity experiments. At low denaturant concentrations a single peak (8.9 S) of the native tetramer is observed. Dissociation results in an additional 3.6S component which we identify as the expanded dimer. No other intermediate is observed. At higher denaturant concentrations only a 1.9S monomer is present. The same results were obtained when the physiological substrates of the enzyme phosphoenolpyruvate and Mg^{2+} were

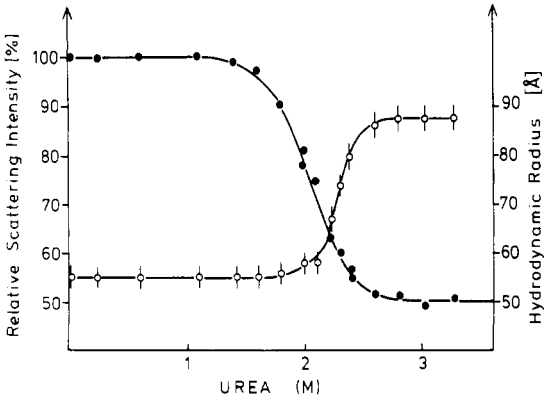

FIGURE 4: Relative scattering intensity (●) and hydrodynamic radius (○) in urea and phosphate buffer (pH 6.5, 5 °C). (—) Theoretical curve calculated according to model 6.

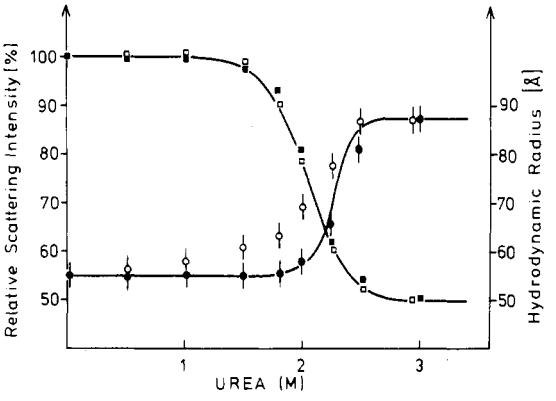

FIGURE 5: Relative scattering intensity (□) and hydrodynamic radius (○) in Tris buffer at pH 8 and 10 °C. The open symbols were obtained without ligands; the filled symbols were obtained from samples which contained 5 mM Mg^{2+} and 2.5 mM phosphoenolpyruvate. (—) Theoretical curve of the results obtained at pH 6.5.

present. In contrast, an analysis of the hydrodynamic parameters at pH 8 yielded different results; especially, we observed an influence of the substrates on the equilibrium of the enzyme.

Although the molecular weight ratio at pH 8 is rather similar to the values obtained at pH 6.5 as indicated by the solid line in Figure 5, in contrast to the experiments at pH 6.5, the Stokes radius is not constant at pH 8 and low denaturant concentrations but increases continuously. Since the molecular weight is not changed under these conditions, it follows that the conformation of the tetramer becomes less compact. It is interesting to note as shown in Figure 5 that this conformational transition is inhibited in the presence of phosphoenolpyruvate and Mg^{2+}. In the latter case one observes similar results as described at pH 6.5 above. Since there is no influence of both ligands on the molecular weight ratio as function of the urea concentration, it follows that the substrates do not change the tetramer–dimer equilibrium. From this, we conclude that again no indication for compact dimer is obtained although we do find a less compact tetramer as a new intermediate in the unfolding pathway.

These results are supported by sedimentation velocity experiments carried out at pH 8 (see Table I). We obtained a single component of 8.4 S at 1.5 M urea instead of 9.1 S in a denaturant-free solution. However, if Mg^{2+} and phosphoenolpyruvate are present, the sedimentation coefficient of the protein in 1.5 M urea is again 9.1 S. At 2.2 M urea two components appear: the 3.6S expanded dimer and 7.4S species of Steinmetz & Deal (1966), the latter one being converted into the 8.8S component if Mg^{2+} and phosphoenolpyruvate

Table I

urea concn (M)	ligand	$s_{20,w}{}^{c}$ (S)
	none	9.1
	5 mM Mg^{2+} and 2.5 mM phosphoenolpyruvate	9.1
1.5	none	8.4
1.5	5 mM Mg^{2+} and 2.5 mM phosphoenolpyruvate	9.1
1.75	none	8.1
1.75	5 mM Mg^{2+} and 2.5 mM phosphoenolpyruvate	8.9
2.2	none	7.4
		3.6
2.2	5 mM Mg^{2+} and 2.5 mM phosphoenolpyruvate	8.8
		3.6
3.3	none	3.5
3.3	5 mM Mg^{2+} and 2.5 mM phosphoenolpyruvate	3.6

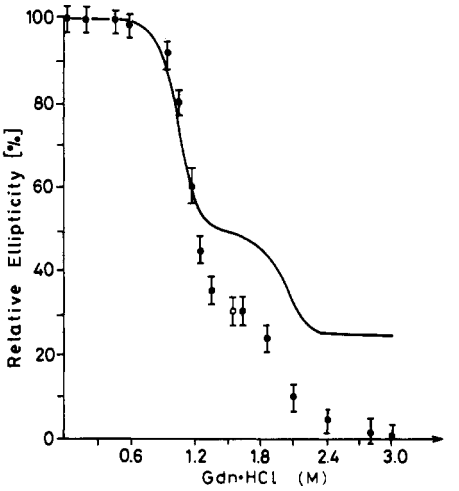

FIGURE 6: Relative scattering intensity and relative value of CD maximum (●) at 222 nm. The measurements were done in phosphate buffer at pH 6.5 and 5 °C. The open symbols were obtained by decreasing and the filled symbols by increasing the Gdn·HCl concentration.

are present. The distribution of the components indicates that the dissociation of the tetramer is not affected by the presence of substrates.

(*c*) *Circular Dichroism.* The changes of the secondary structure obtained from the ellipticity maximum at 222 nm are related to the changes of the molecular weight. This is shown in Figure 6. The main decrease of the ellipticity occurs at 1 M Gdn·HCl parallel to the formation of the dimer. Again a plateau is observed, and this suggests that the expanded dimer is to a large extent but not completely, disordered. The monomer has no secondary structure. The same ellipticity values are observed by either increasing or decreasing the concentration of guanidine hydrochloride above 1.5 M. Further dilution of the denaturant yields only partial recovery of the signal probably due to the formation of random aggregates. The figure also shows the molecular weight ratio for comparison.

(*d*) *Fluorescence.* The fluorescence intensities of the protein in Gdn·HCl and urea coincide if they are plotted on an appropriate concentration scale (Figure 7). Urea is less efficient than Gdn·HCl but induces the same structural changes. The fluorescence enhancement at low concentrations of denaturant reflects a conformational change of the tetramer. The subsequent quenching of the fluorescence at 1 M Gdn·HCl or 2 M urea runs parallel to the change of the molecular weight ratio. Decreasing or increasing the concentrations of the denaturant at a protein concentration of 0.03 mg/mL dem-

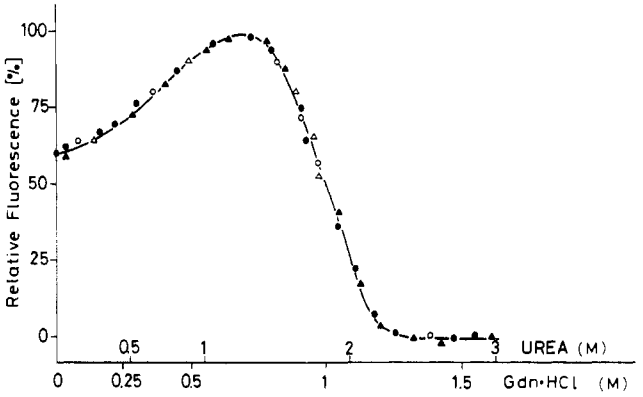

FIGURE 7: The relative intensity of the fluorescence maximum in Gdn·HCl (●) and urea (▲) at pH 7 and 5 °C. Filled symbols were obtained by increasing and open symbols by decreasing the denaturant concentration. (—) Theoretical curve obtained from model 6.

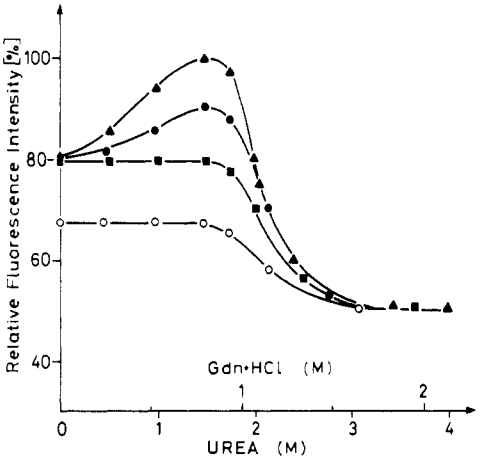

FIGURE 8: Relative fluorescence intensity at pH 8 in urea (△), at pH 6.5 in Gdn·HCl (○), at pH 8 in urea and the presence of 5 mM Mg^{2+} and 2.5 mM phosphoenolpyruvate (■), and at pH 8 in Gdn·HCl and in the presence of 30 mM Mg^{2+} and 15 mM phosphoenolpyruvate (●). All measurements were done in Tris buffer and at 20 °C.

onstrates the complete reversibility of the transition curve. This together with the observations of the hydrodynamic properties, shows the reversibility of the overall transition from the native tetramer to the monomer. More concentrated solutions of the protein, however, give only partial recovery of the signal. This demonstrates the critical role of the protein concentration in the process of renaturation of the oligomeric enzyme. No information is obtained from the fluorescence data concerning the dissociation of the dimer.

Figure 8 shows the influence of pH and the ligands on the fluorescence signal. A fluorescence increase is observed between pH 7 and pH 8 but not at pH 6.5. The increased intensity of the signal and the bathochromic shift in urea can be reversed if Mg^{2+} (5 mM) and PEP (2.5 mM) or alanine (10 mM) is added (see Discussion). By contrast, the fluorescence enhancement induced by Gdn·HCl is only partially reversible even at high concentrations of Mg^{2+} (30 mM) and PEP (15 mM).

(*e*) *Enzyme Activity.* The activity measurements were carried out with two different methods. In the first method the enzyme was incubated at a specific concentration of denaturant. Then, the sample was diluted and the activity immediately determined in a coupled enzyme assay. The procedure yields a minimum estimate of the enzymic activity. From Figure 9 it is evident that in both cases, in urea as well as in Gdn·HCl, dissociation and deactivation run parallel. Both reactivation by reassociation and a significant contribution by

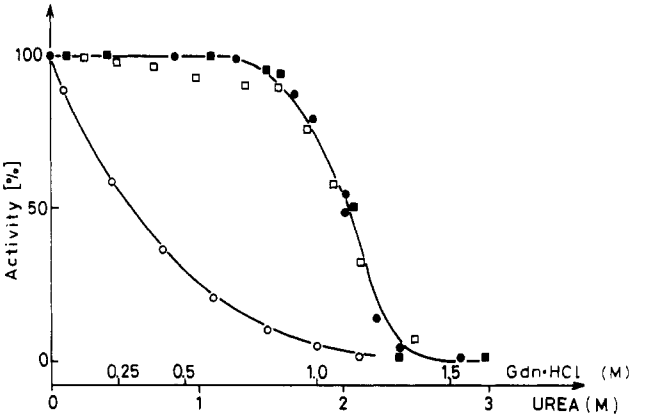

FIGURE 9: Enzyme activity measurements obtained from the coupled procedure (conditions are given under Materials and Methods) at pH 6.5 and 5 °C in Gdn·HCl (●) and urea (■). pH-stat measurements at pH 8 in Gdn·HCl (○) and urea (□) at 20 °C.

a possible compact dimer to the observed activity can be excluded by these experiments. However, a fast reversible inactive state at low denaturant concentrations cannot be excluded by this technique.

An analysis of the enzyme activity with the pH-stat method in the presence of urea yielded the same results as given above. In the presence of Gdn·HCl, however, the activity was found to decrease continuously with increasing Gdn·HCl concentrations. From this we conclude that a fast reversible inactive state of the tetramer must exist.

Discussion

The solvent denaturation study of pyruvate kinase reveals three reversible structural transitions. With increasing concentration of denaturant the native tetramer is first transformed into a less compact and inactive state. This is followed by dissociation into partially folded dimers with disordered monomers being formed at high concentrations of denaturant. Although it is less efficient, urea induces the same structural changes as Gdn·HCl. The transition curves of both denaturants coincide on an appropriate concentration scale.

The conformational change of the tetramer which is observed above pH 7 enhances the protein fluorescence. A very similar effect is obtained by phenylalanine, an inhibitor of pyruvate kinase. Like Gdn·HCl and urea, phenylalanine increases the fluorescence of the enzyme by 20% above pH 7. At pH 6.5 no effect is found in both systems, and phenylalanine no longer inhibits the enzyme activity (Carminatti et al., 1971; Kayne & Price, 1972). The fluorescence enhancement we observed in the urea system can be completely reversed by Mg^{2+} and phosphoenolpyruvate or alanine. Similarly, the fluorescence saturation curve of phenylalanine becomes sigmoidal if phosphoenolpyruvate and Mg^{2+} are added and is shifted to higher phenylalanine concentrations. Alanine reverses also the fluorescence enhancement.

These data are in reasonable agreement with the inhibition of the activity by phenylalanine (Carminatti et al., 1971; Kayne & Price, 1972). No inhibition of the activity is found in the urea system because phosphoenolpyruvate and Mg^{2+}, being necessary for the activity assay, renature the enzyme. However, inhibition is observed when the conformational change is induced by Gdn·HCl, being only partially reversed by phosphoenolpyruvate and Mg^{2+}.

Mn^{2+} binding studies (Kayne & Price, 1972) reveal that phenylalanine weakens the affinity of the divalent metal binding site of the enzyme by a factor 3.5. The enhancement of the NMR proton relaxation rate of water by bound Mn^{2+}

is not significantly changed by phenylalanine. This suggests that no major changes occur in the environment of bound Mn^{2+} and that the phenylalanine site can be considered as distinct from the active site. The effect of urea on the divalent cation binding site of rabbit muscle pyruvate kinase was studied by Cottam & Mildvan (1971). Their most obvious result was that urea like phenylalanine has little effect on the enhancement of the proton relaxation rate of water and the number of Mn^{2+} binding sites up to 2 M. However, the dissociation constant of Mn^{2+} between 0 and 1.6 M urea increases by a factor of 5.

An explanation for this correspondence may be that specific effects by ligands and nonspecific effects of the denaturants are linked via the protein–solvent interaction. The charge difference of Gdn·HCl and urea may be responsible for the different result in the presence of phosphoenolpyruvate and Mg^{2+}. Despite the striking similarities, we do not consider the conformation changes induced by phenylalanine and the denaturants as completely identical, because no hydrodynamic effect of phenylalanine is observed.

At low concentrations of denaturant both the increase of the hydrodynamic radius and the enhancement of the fluorescence suggest that both structural parameters record the same conformational change. The common pH dependence and the reversibility induced by phosphoenolpyruvate and Mg^{2+} further support this proposition. The activity measurements in the presence of Gdn·HCl show that the less compact tetramer has no enzymic activity.

The quenching of the protein fluorescence around 1 M Gdn·HCl and 2 M urea coincides with the tetramer–dimer dissociation curve. However, it has to be noted that the fluorescent transition curve is slightly shifted (by ~0.1 M Gdn·HCl) to lower denaturant concentrations due to the low protein concentration of 0.03 mg/mL relative to the curve obtained by light-scattering measurements at 1 mg/mL. After a concentration correction (Herskovits et al., 1978) both curves obtained from fluorescence and light-scattering measurements coincide. Under these conditions, the whole transition curve is completely reversible.

The dimer–monomer dissociation is reversible even at a protein concentration of 1 mg/mL. It is known that solvent denaturation of pyruvate kinase is overall reversible, since Cottam et al. (1969) found that a tetramer with the same sedimentation and diffusion coefficients as the native enzyme can be regained from Gdn·HCl- and urea-denatured monomers. Recovery of the enzyme activity up to 80% was reported (Steinmetz & Deal, 1966; Cottam et al., 1969). Our results clearly show that the transition curves are also point by point reversible.

Our experiments also indicate the existence of a stable dimer. Stable dimers were found in other tetrameric proteins such as hemoglobin (Herskovits et al., 1978) or phosphofructokinase (Parr & Hammes, 1975). Stable dimers imply that there are at least two different intersubunit contact areas with different binding energies. While acid-denatured aldolase dissociates completely without a stable intermediate (Rudolph et al., 1978), the Gdn·HCl denaturation profile looks similar to that of pyruvate kinase. The fluorescent intensity increases below 1 M Gdn·HCl, and above 1 M also two transitions of the spectral properties are observed (Gerschitz et al., 1977).

In agreement with observations on most other oligomeric enzymes (Jaenicke, 1978), pyruvate kinase also requires association for full enzymic activity. Deactivation and dissociation of the tetramer into dimer strictly coincide. In contrast, Steinmetz & Deal (1966) and Cottam et al. (1969) report a 7.2S compact dimer which is fully or partially active. We confirm the sedimentation data and activity measurements given by these authors; however, our conclusion is different. From the molecular weight dependency of the sedimentation coefficient in the case of compact molecules, one expects that 8.9S tetramers yield 5.6S compact dimers. The large difference (7.2 S instead of 5.6 S) is difficult to explain. Furthermore, we do not observe a sharp transition, but a continuous decrease of the sedimentation coefficient with increasing urea concentrations. However, the diffusion coefficient decreases in a similar way so that the s/D value and therefore the molecular weight remains constant. The molecular weight ratio obtained from light-scattering measurements also remains constant in this concentration range. Our conclusion is that the so-called 7.2S intermediate is a partially expanded tetramer and not a compact dimer. Furthermore, the 7.2 S intermediate is reconverted into the 8.8S species in the presence of Mg^{2+} and phosphoenolpyruvate without any change of the s/D value or the molecular weight ratio. This explains why these authors found enzymic activity of the 7.2S species.

The observed dimer, which we identify with the 3.6S intermediate, is partially unfolded and not active. For the existence of a partially unfolded state we invoke the following reasoning. The factors which influence the hydrodynamic size of a macromolecule are obtained from the frictional ratio. The frictional ratio of the molecule can be calculated from

$$R_h/R_d = f/f_0[(v_2 + d)/v_2]^{1/3} \quad (4)$$

The dry radius R_d is given by

$$R_d = (3Mv_2/4N)^{1/3} \quad (5)$$

f/f_0 is a shape factor, v_2 is the partial specific volume, M is the molecular weight, N is Avogadro's number, and d is the hydration volume of the protein. The tetramer has a frictional ratio of 1.34, while the expanded dimer gives 2.54. Changes of the molecular shape cannot explain this large increase of the frictional ratio. A 20-fold increase of the axial ratio of the corresponding ellipsoid has to be assumed (Scheraga, 1961). Similarly, the specific volume usually changes less than a few percent upon denaturation (Richards, 1977). The main contribution must therefore come from an increased amount of solvent associated with the protein by exposure of hydrophobic groups and less structure.

The amount of structure of the dimer and monomer can be estimated by consideration of the Stokes radius and the intrinsic viscosity. The native tetramer has an intrinsic viscosity of 4.5 cm^3/g, a value which is typical for a globular protein. The expanded dimer has a viscosity of 45 cm^3/g in 1.5 M Gdn-HCl and a Stokes radius of 84 Å; a random coil with a molecular weight of 120 000 would be expected to have the values of 64 cm^3/g for the intrinsic viscosity (Tanford, 1966) and 94 Å for the Stokes radius (Rao et al., 1974). However, the monomer has values of 49 cm^3/g and 67 Å for these constants, respectively. This is consistent with a random-coiled protein with a molecular weight of 60 000. From these hydrodynamic experiments it follows that the expanded dimer is partially ordered whereas almost complete unfolding has occurred at the monomer state. The conclusions are further supported by the ellipticity changes. The expanded dimer has lost ~70% of its secondary structure.

In order to relate the observed intermediates to the structure of the enzyme, one has to keep in mind that the unfolding pathway of pyruvate kinase starts with a conformational change which can be reversed by Mg^{2+} and phosphoenolpyruvate and which does not influence the association–dissociation equilibrium of the enzyme. The subsequent two dis-

sociation steps are accompanied by a partial unfolding of the secondary structure. This partial unfolding is simply explained by a domain concept. The subunits of the tetramer should consist of three domains. Only two of them should be in contact with neighboring subunits of the oligomer. This model is supported by the X-ray structure.

The presented data do not provide a detailed structural description of the observed intermediates. However, from the X-ray structure (Stammers & Muirhead, 1975; Levine et al., 1978), it is evident that the protein is not homogeneous but each subunit is folded into three distinct domains. Two of them form intersubunit contact areas. The two subsequent dissociation processes of the tetramer and dimer may reflect the sequential unfolding of these domains. Since the two domains differ in size, it is likely that the larger one unfolds first because the major changes of the structural parameters occur when the expanded dimer is formed. The conformational change of the tetramer may involve the third domain which is not in contact with neighboring subunits. For substantiation of this hypothesis, the location of the tryptophan residues has to be known.

Thermodynamic Model

Solvent denaturation of muscle pyruvate kinase allowed us to identify four distinct and reversible states of the unfolding pathway: two tetrameric conformers, a partially folded dimer, and a complete disordered monomer. In order to analyze the transition curves on a quantitative basis, we suggest a thermodynamic model, which should simultaneously fit the elastic and quasi-elastic light-scattering data and the fluorescence and activity measurements:

$$A_4 \rightleftharpoons A_4^* \rightleftharpoons 2A_2 \rightleftharpoons 4A \tag{6}$$

We assume that no further intermediates are present in significant concentrations.

The equilibrium constants and the free energy changes are obtained from the light-scattering data as follows. The observed scattering intensity I_{av} (eq 1) is a concentration-weighted average of the individual intensities of species i defined by the model:

$$\frac{I_{av}}{I_0} = \frac{\sum_i C_i M_i^2}{C_0 M_0^2} = \frac{K M_w}{M_0} \tag{7}$$

C_i is the molar concentration of species i and M_w is the weight average. K is an optical constant.

Quasi-elastic light scattering measures the z-average diffusion coefficient:

$$D^z = \sum_i C_i M_i^2 D_i / \sum_i C_i M_i^2 \tag{8}$$

M_i is the molecular weight, and D_i is the diffusion coefficient of species i. The average radius is then calculated from

$$1/R = \sum_i (C_i M_i^2 / R_i) / \sum_i C_i M_i^2 \tag{9}$$

The equilibrium constants are obtained from the molar concentrations according to the model (6):

$$K_1 = (C_4^*/C_4) \qquad K_2 = (C_2^2/C_4^*) \qquad K_3 = C_1^2/C_2 \tag{10}$$

The change of the chemical potential of transition 1 is related to the equilibrium constant K_1 by

$$\Delta\mu_1 = -RT \ln K_1 \tag{11}$$

This equation allows the determination of the free energy changes in the presence of denaturant. However, a sizable extrapolation to zero denaturant concentration has to be applied to obtain an estimate of the stability of the protein under physiological conditions.

The standard approach to this problem is a multiple binding model, assuming that the denaturant agents are preferentially bound to the unfolded form of the molecule (Tanford, 1968). However, the narrow denaturant concentration range which is usually available to determine equilibrium constants often allows data fitting with large variations of the model parameters (Pace, 1975). This is especially the case for pyruvate kinase. Furthermore, the definition of binding is rather difficult in a solution in which the ligand occupies a large part of the volume. We adopt here a more general thermodynamic approach, which was developped recently by Schellman (1978) and which includes the stoichiometric binding model as a special case.

The standard chemical potential of a component j in solution can be written on a molar scale as

$$\mu j = \mu_j^0 + RT \ln C_j + RTb_j \tag{12}$$

The indices in a three-component solution are different by convention as follows: $j = 1$, the principal solvent, water; $j = 2$, the macromolecule; $j = 3$, small-molecule solute components such as Gdn·HCl or urea. μ_j^0, C_j, and RTb_j are respectively the chemical potential of the reference state, the molarity, and the excess free energy. b_j vanished only in the limit that all $C_{j>1}$'s go to zero.

The free energy change between two forms of the macromolecule is then given by

$$\Delta\mu_2 = \Delta\mu_2^0 + RT\Delta b_2^0 \tag{13}$$

The index 0 of Δb_2^0 indicates that eq 13 is valid in the limit of low C_2. $\Delta\mu_2^0$ is the desired change of the chemical potential in the absence of solutes.

The excess free energy functions for a solution component can be represented by a Taylor series in all solute concentrations:

$$b_j^0 = \sum_k b_{jk}^0 C_k + \sum_{k,n} b_{jkn}^0 C_k C_n + \ldots \tag{14}$$

b_{jk}^0 and b_{jkn}^0 are partial derivatives of b_j in the limit of zero concentrations of all solutes.

Following Schellman (1978), we consider a solution model, in which b_2 is linear in the concentration of component 3. In the limit of low concentrations of components 2 we have

$$b_2^0 = b_{23}^0 C_3 \tag{15}$$

and the change of the chemical potential is obtained by combination of eq 13 and 15:

$$\Delta\mu_2 = \Delta\mu_2^0 + RT\Delta b_{23}^0 C_3 \tag{16}$$

Although this linear model is very simple, it was found to be valid for a number of proteins (Greene & Pace, 1974; Herskovits et al., 1978; Maruyama et al., 1977; Ahmad & McPhie, 1978; Kanehisa & Ikegami, 1977). Its consistency can be tested by using different denaturants which should extrapolate to the same free energy change. We used the linear extrapolation procedure to analyze the urea and Gdn·HCl denaturation of pyruvate kinase.

The multistate equilibrium as it is defined by the model involves the solution of a polynomial obtained numerically by a linear regression analysis. The stability of the least-squares minimum was tested by several computer cycles with different initial values. The unambiguous solution is obtained because

Table II: Thermodynamic Data of Rabbit Muscle Pyruvate Kinase

denaturant:	Gdn·HCl		urea		
transition	$\Delta\mu_2^0$ (kcal/mol)	$RT\Delta b_{23}^0$ [kcal/(mol·M)]	$\Delta\mu_2^0$	$RT\Delta b_{23}^0$	k_i
A_4---A_4*	1.65	5	1.6	2.7	5×10^{-2}
A_4*-$2A_2$	15.9	9.3	16.3	4.7	2×10^{-13}
A_2-$2A_1$	15.6	4.5			5×10^{-13}

transitions are well separated. The optimal parameter set is given in Table II.

The conformational transition of the tetramer and the small free energy change of 1.6 kcal/M indicates that the molecule is flexible. The equilibrium is easily shifted by various ligands. The stability of the tetramer against dissociation (16 kcal/M) is comparable to that of desoxihemoglobin (14 kcal/M) (Mills & Ackers, 1979). It also compares well with the stability of small monomeric proteins in urea and Gdn·HCl (Greene & Pace, 1974).

The resulting dissociation constant of 10^{-13} M and the low stability of the compact dimer exclude dissociation as a functional mode of the enzyme. The stability of the dimer is very similar. However, the efficiency parameter of the dimer monomer transition is much lower. The Gdn·HCl efficiency parameters of the A_4–A_4* [5.0 kcal/(mol·M)] and A_2–A_1 [4.5 kcal/(mol·M)] transitions are comparable to values of chymotrypsin (M_r 25 000) [4.1 kcal/mol·M)] (Greene & Pace, 1974) and phosphoglycerate kinase (M_r 45 000) [5.8 kcal/(mol·M)] (Burgess & Pain, 1977). According to Burgess and Pain, however, the 5.8 kcal/(mol·M) represents only half of the molecule, because the two domains of phosphoglycerate kinase unfold separately.

A theoretical efficiency parameter of the total unfolding of pyruvate kinase in 1 M Gdn·HCl can be calculated with the method of Greene & Pace (1974), using the amino acid composition (Cottam et al., 1969), the amino acid transfer data of Nozaki & Tanford (1970), and Tanford's relation (Tanford, 1970):

$$\Delta G_{app} = \Delta G_{app}^0 + 0.3\sum_i n_i \Delta g_{tr,i} \qquad (17)$$

$\Delta g_{tr,i}$ is the free energy of transfer of group i from water to 1 M Gdn·HCl, n_i is the number of groups of type i, and 0.3 represents an average value of the fractional change in exposure to the solvent for all groups which are not already fully exposed in the native state.

The calculated efficiency parameter in 1 M Gdn·HCl is 19.6 kcal/(mol·M), whereas the experimental value of A_4*–A_2 transition at 1 M Gdn·HCl is considerably smaller, namely 9.3 kcal/(mol·M). Even if one assumes independent unfolding of the subunits, one has to conclude that either the theoretical method is not appropriate or that dissociation of the tetramer exposes only part of the buried groups to the solvent. The efficiency ratio of the ionic denaturant Gdn·HCl and the nonionic urea b_{23}^G/b_{23}^U (1.98) is similar to those observed for lysozyme (1.68), chymotrypsin (1.98), and lactoglobulin (1.84). These proteins are stabilized mainly by hydrophobic contacts. Ribonuclease, a relatively polar protein, has a ratio of 2.82 (Greene & Pace, 1974). Polar interactions seem not to play a dominant role for the stability of the tetrameric pyruvate kinase.

Acknowledgments

We thank K.-H. Müller and Dr. Th. Plesser for the help with the computer programs and R. Müller and U. Schacknies for their excellent technical assistance. Furthermore, helpful discussions and contributions of hitherto unpublished results by Dr. T. Reed are gratefully acknowledged. Especially, we would like to thank Professor D. Wetlaufer for his multiple discussions and helpful contributions in the initiation of our folding studies and his help over the years.

References

Ahmad, F., & McPhie, P. (1978) *Biochemistry 17*, 241–246.
Burgess, R. J., & Pain, R. H. (1977) *Biochem. Soc. Trans. 5*, 652–654.
Carminatti, H., Jimenez, L., Leiderman, B., & Rozengurt, E. (1971) *J. Biol. Chem. 246*, 7284–88.
Cottam, G. L., & Mildvan, A. S. (1971) *J. Biol. Chem. 246*, 4363–4365.
Cottam, G. L., Hollenberg, P. F., & Coon, M. Y. (1969) *J. Biol. Chem. 244*, 1481–1486.
Creighton, Th. E. (1978) *Prog. Biophys. Mol. Biol. 33*, 231–297.
Cummins, H. Z. (1973) *NATO Adv. Study Inst. Ser., Ser. B 3*, 285–330.
Doster, W., & Hess, B. (1978) *Hoppe-Seyler's Z. Physiol. Chem. 359*, 1043–1044.
Dubin, S., B., Feher, G., & Benedek, G. B. (1973) *Biochemistry 12*, 714–720.
Gerschitz, J., Rudolph, R., & Jaenicke, R. (1977) *Biophys. Struct. Mech. 3*, 291–302.
Greene, R. F., & Pace, N. (1974) *J. Biol. Chem. 249*, 5388–5393.
Herskovits, T. T., George, R. C. S., & Cavanagh, S. M. (1978) *J. Colloid Interface Sci. 63*, 226–234.
Jaenicke, R. (1978) *Naturwissenschaften 65*, 569–577.
Johnson, G. S., Steinmetz Kayne, M., & Deal, W. C. (1969) *Biochemistry 8*, 2455–2462.
Kanehisa, M. I., & Ikegami, A. (1977) *Biophys. Chem. 6*, 131–149.
Kayne, F. J., & Price, N. C. (1972) *Biochemistry 11*, 4415–4420.
Kielley, W. W., & Harrington, W. F. (1960) *Biochim. Biophys. Acta 41*, 401–421.
Levine, M., Muirhead, H., Stammers, D. K., & Stuart, D. I. (1978) *Nature (London) 271*, 626–630.
Maruyama, S., Kuwajima, K., Nitta, K., & Sugai, S. (1977) *Biochim. Biophys. Acta 494*, 343–353.
Mills, C. F., & Ackers, G. K. (1979) *Proc. Natl. Acad. Sci. U.S.A. 76*, 273–277.
Noelken, M. E., & Timasheff, S. N. (1967) *J. Biol. Chem. 242*, 5080–5085.
Nozaki, Y., & Tanford, Ch. (1970) *J. Biol. Chem. 245*, 1646–1652.
Pace, N. C. (1975) *CRC Crit. Rev. Biochem. 3*, 1–43.
Parr, G. R., & Hammes, G. G. (1975) *Biochemistry 14*, 1600–1605.
Pusey, P. N., Koppel, D. E., Schaefer, D. W., & Camerini-Otero, R. D. (1974) *Biochemistry 13*, 952–960.
Rao, S. P., Carlstrom, D. E., & Miller, W. G. (1974) *Biochemistry 13*, 943–952.
Richards, F. (1977) *Annu. Rev. Biophys. Bioeng. 6*, 151–176.
Rudolph, R., Haselbeck, A., Knorr, F., & Jaenicke, R. (1978) *Hoppe-Seyler's Z. Physiol. Chem. 359*, 867–871.
Schellman, J. A. (1978) *Biopolymers 17*, 1305–1322.
Scheraga, H. A. (1961) in *Protein Structure*, pp 1–10, Academic Press, New York and London.
Stammers, D. K., & Muirhead, H. (1975) *J. Mol. Biol. 95*, 213–225.

Steinmetz, M. A., & Deal, W. C. (1966) *Biochemistry 5*, 1399-1405.
Tanford, Ch. (1966) *J. Biol. Chem. 241*, 1521-23.
Tanford, Ch. (1968) *Adv. Protein Chem. 23*, 121-182.
Tanford, Ch. (1970) *Adv. Protein Chem. 24*, 1-95.
Timasheff, S. N., & Townend, R. (1970) in *Physical Principles and Techniques of Protein Chemistry* (Leach, S. I., Ed.) Part B, pp 147-212, Academic Press, New York.

Internal Motions in Myosin. 2†

Stefan Highsmith* and Oleg Jardetzky

ABSTRACT: The high-resolution ^1H NMR detected internal motions in myosin and myosin subfragment 1 (S1) [Highsmith, S., Akasaka, K., Konrad, M., Goody, R., Holmes, K., Wade-Jardetzky, N., & Jardetzky, O. (1979) *Biochemistry 18*, 4238-4244] were unperturbed by induced changes in the rate of protein tumbling, and the mobile regions proved inaccessible to added surface-directed paramagnetic probes. The rate of tumbling was changed by changing the solvent viscosity for S1 or by aggregation to thick filaments for myosin. Neither manipulation caused a measurable broadening of the narrow lines in the spectrum. Sulfhydryl-directed covalently attached nitroxide spin-labels, soluble nitroxide spin-labels, and $MnCl_2$ were used to probe the surface. Unique labeling at the fastest reacting thiol of S1 had no effect on the NMR spectrum. Multiple labeling of thiols caused a small but detectable broadening of the narrow peaks. Soluble spin-labels and $MnCl_2$ had a very small effect on the narrow bands even in great excess. The results substantiate the notion that myosin has internal motions that are independent of the overall rate of rotation and suggest that the mobile structure is mainly in the interior of the S1 moiety. This supports a model in which actin quenches the internal motions of myosin by changing the structure of myosin upon binding.

Force generation in muscle by the actomyosin-nucleotide complex very likely involves a substantial change in the overall dimensions of the complex. Most contemporary working hypotheses stem from the original cross-bridge models of Huxley (1969) and Huxley & Simmons (1971). In the simplest versions, actin and myosin reorient relative to one another without either individual protein changing its structure. Another possibility is that actin and/or myosin themselves undergo a structural change as part of the total conformational change of the complex. Thus far, no evidence has been obtained to demonstrate any structural changes. Recently, a change in the dynamics of myosin due to actin binding was reported which is large enough to suggest a possible structural change for myosin when it binds actin (Highsmith et al., 1979). It was shown by high-resolution ^1H NMR[1] measurements that more than 20% of the structure of subfragment 1 (S1) of rabbit skeletal myosin is undergoing rapid internal motion. Neither MgATP nor a selection of its analogues appeared to have any effect on the internal motions. However, when actin was bound to S1, it caused the narrow peaks associated with the mobile structure to disappear. Small perturbations in the rate of free S1 rotation in solution had no effect on the narrow peaks in its spectrum. Therefore, it was suggested that actin binding eliminated the narrow NMR peaks of S1 because it changed the structure of S1 in such a way as to quench its internal motions. However, the possibility that the loss of narrow peaks was due to the trivial mechanism of a reduced rate of overall molecular rotation was not eliminated. The location of the mobile structure in S1 was also not identified beyond the exclusion of the nucleotide binding site and the homologous parts of the alkali light chains. In particular, the possibility that the mobile 20% of S1 was composed of amino acid side chains on the surface was not to be eliminated.

Two experimental approaches to this problem are reported here. First, the rate of rotation of S1 was reduced without actin to determine how much of the actin binding effect is due to the slowing of the overall rotation of S1. Second, paramagnetic probes were used to estimate the fraction of the mobile structure accessible to the solvent and therefore presumed to be on the surface of the protein. The results of these experiments indicate that the rate of rotation of S1 has very little effect on the line widths of the narrow resonance peaks. In addition, it appears that almost all of the mobile structure is inaccessible to small solute molecules in the solvent. These results indicate that the "internal motions" occur in the interior of the protein and that actin quenches the internal motions when it binds by altering a substantial part of the structure of S1.

Experimental Section

Materials. Myosin was prepared from dorsal muscle of New Zealand rabbit by the method of Nauss et al. (1969) and purified by $(NH_4)_2SO_4$ fractionation. Its concentration in solution was determined by using the constants $M_r = 450\,000$ and $\epsilon^{1\%}_{280nm} = 5.7$. S1 was prepared from myosin by the method of Weeds & Taylor (1975) and purified as a mixture of isozymes by $(NH_4)_2SO_4$ fractionation. S1 prepared this way has

† From the Stanford Magnetic Resonance Laboratory, Stanford University, Stanford, California 94305. *Received December 14, 1979; revised manuscript received October 2, 1980.* This work was supported by National Science Foundation Grant GP23633 and Grants RR00711 and 1R01AM25177. S.H. is the recipient of National Institutes of Health Research Career Development Award 1K04AM00509.

* Correspondence should be addressed to this author at the Department of Biochemistry and Laboratory of Physiology and Biophysics, School of Dentistry, University of the Pacific, San Francisco, CA 94115.

[1] Abbreviations used: NMR, nuclear magnetic resonance; S1, myosin subfragment 1; ATP, adenosine 5'-triphosphate; Tempo-IAA, 4-[(2-iodoacetyl)amino]-2,2,6,6-tetramethylpiperidinyl-1-oxy; Tempop, 4-hydroxy-2,2,6,6-tetramethylpiperidinyl-1-oxy dihydrogen phosphate (ester); HSA, human serum albumin.

0006-2960/81/0420-0780$01.00/0